



Fermi National Accelerator Laboratory

FERMILAB-Pub-81/42-EXP
7340.448
(Submitted to Phys. Rev. Lett.)

OBSERVATION OF SHADOWING IN THE VIRTUAL PHOTON TOTAL HADRONIC CROSS SECTION ON NUCLEI

M. S. Goodman, M. Hall, W. A. Loomis,
F. M. Pipkin, and R. Wilson
High Energy Physics Laboratory
Harvard University
Cambridge, Massachusetts 02138 USA

R. K. Thornton
Tufts University
Medford, Massachusetts 02155 USA

R. Hicks and T. Kirk
Fermi National Accelerator Laboratory
Batavia, Illinois 60510 USA

J. Macallister and T. Quirk
Nuclear Physics Laboratory
Oxford University
Oxford, England OX1 3RH

S. C. Wright
Physics Department
The University of Chicago
Chicago, Illinois 60637 USA

G. Brandenburg and C. Young
Massachusetts Institute of Technology
Cambridge, Massachusetts 02139 USA

and

W. R. Francis and I. Kostoulas
Michigan State University
East Lansing, Michigan 48823 USA

May 1981



Observation of Shadowing in the Virtual Photon Total Hadronic
Cross Section on Nuclei

M.S. Goodman, M. Hall^o, W.A. Loomis, F.M. Pipkin, and R. Wilson
High Energy Physics Laboratoryⁱ
Harvard University
Cambridge, Massachusetts 02138

R.K. Thornton
Tufts University[†]
Medford, Massachusetts 02155

R. Hicks[~] and T. Kirk
Fermilab[†]
Batavia, Illinois 60510

J. Macallister and T. Quirk^Δ
Nuclear Physics Laboratory^{*}
Oxford University
Oxford, England OX1 3RH

S.C. Wright **
Physics Department
The University of Chicago
Chicago, Illinois 60637

G. Brandenburg^η and C. Young[§]
Massachusetts Institute of Technology[†]
Cambridge, Massachusetts 02139

W.R. Francis[£] and I. Kostoulas^{††}
Michigan State University^{**}
East Lansing, Michigan 48823

Abstract

We have measured the total hadronic cross section of virtual photons incident on carbon, copper and lead in the region $Q^2 = (0.01 - 30.) \text{ GeV}^2$ and $\nu = (40 - 200) \text{ GeV}$. A 209 GeV/c muon beam was used as a source of virtual photons. The results indicate shadowing of the virtual photons below $Q^2 = 1 \text{ GeV}^2$ and a decrease of shadowing for $Q^2 > 3 \text{ GeV}^2$. The shadowing persists to larger Q^2 than indicated by experiments at lower ν .

The phenomenon of shadowing has been reported for both real and virtual photons incident on nuclei.¹ Shadowing is the less than linear increase of the total hadronic cross section with nucleon number A , as if part of the nuclear matter were casting a shadow on the remainder. The magnitude and dependence of the shadowing on the virtual photon mass squared (Q^2) has been controversial,² and shadowing has been previously studied for only low energy virtual photons ($\nu \lesssim 15$ GeV). The amount and kinematic behavior of the virtual photon shadowing allows us to study the transition between the two extreme pictures of photon interactions with nucleons; namely the hadronic picture, which describes the interaction of real and low Q^2 virtual photons, and the quark-parton model which describes the interaction of high Q^2 virtual photons.² We have measured the Q^2 dependence of the shadowing of virtual photons and extended the measurements to much larger virtual photon energy than previous experiments.

The experiment was performed using the Chicago Cyclotron Magnet Spectrometer³ at Fermilab with a 209 GeV/c negative muon beam as a source of virtual photons. Muons were scattered on targets of carbon, copper and lead, and also from an empty target for background measurements. The target thicknesses were 20.43 gm/cm^2 for carbon, 19.78 gm/cm^2 for copper, and 9.73 gm/cm^2 for lead. The CCM spectrometer (Figure 1) was modified by the addition of a lead glass shower counter array, to improve the separation of hadronic events from electromagnetic background events. The event trigger consisted of a coincidence between an incident muon signal in the beam defining scintillators (BS), a scattered muon signature in the downstream

hodoscopes (a coincidence between an M counter and a G or H counter) and no signal in the downstream beam veto (V). The total muon flux was approximately 2.5×10^9 on each of the carbon and copper targets, and 4.7×10^9 on the lead target.

The analysis consisted of identifying the hadronic events and separating them from the electromagnetic background. Events were reconstructed using procedures developed for earlier experiments with this apparatus.³ The procedure for hadronic event identification utilized the large typical transverse momentum squared of hadron secondaries, with respect to the virtual photon direction^{4,5} $\langle p_t^2 \rangle \sim 0.18 \text{ (GeV/c)}^2$. This is larger than the $\langle p_t^2 \rangle$ of secondaries in the more numerous electromagnetic background events due to the wide angle bremsstrahlung process² (WAB), which is typically 0.01 (GeV/c)^2 . The data were divided into regions based on the expected shower positions from WAB photons. Events with expected shower positions outside the lead glass aperture (events with $\nu < 110 \text{ GeV}$ and $Q^2 > 3 \text{ (GeV)}^2$) were assumed to be hadronic, and a calculated WAB correction was made (average $< 2\%$ all targets). For events within the lead glass aperture, hadronic event classification was based on a variety of criteria developed from earlier studies of hadronic secondaries in this apparatus on hydrogen.

Hadronic events were required to satisfy at least

one of the following criteria a) Average (P_t^2) of secondary tracks $> 0.03 \text{ (GeV/c)}^2$, b) showers in the lead glass array displaced out of the bending plane from the expected impact position for a WAB photon, c) rms angular spread of spark chamber hits upstream of the spectrometer magnet $> 15 \text{ mrad}$ with no secondary tracks downstream or detected showers. Hadronic event candidates which satisfied only one of the above conditions were further required to have a total energy deposition in the lead glass array of $< 70\%$ of the virtual photon energy. These event selection cuts were studied using Monte Carlo simulations of hadronic and electromagnetic events which were analyzed with the same procedures as the real data. The Monte Carlo calculations were based on the measured hadron distributions on hydrogen⁴ and incorporated showering of π^0 photons using the EGS code system.⁶

The total cross section for virtual photons is taken from the muon scattering cross section as:

$$\sigma(Q^2, A) = \frac{1}{\Gamma} \left(\frac{d^2\sigma_\mu}{dQ^2 dv} \right) \quad (1)$$

where Γ is the effective flux of virtual photons created by the muon. To obtain the hadronic cross sections, the data were corrected for losses of hadronic events due to event selection cuts. These corrections were determined from ratios of event classes in the data, and checked using the Monte Carlo calculations.

Figure 2 shows $\frac{\bar{\sigma}(Q^2, A)}{A}$ for the respective targets and Q^2 ranges.

The data were binned in the Q^2 region below 3 GeV^2 from $\nu = (110-200) \text{ GeV}$. For the region above 3 GeV^2 to improve statistics the data were binned from $\nu = (40 - 200) \text{ GeV}$.

The data have been corrected for the muon acceptance of the apparatus ($>20\%$ over the kinematic region covered), muon beam reconstruction efficiency ($>70\%$), the loss of hadronic events ($17 \pm 5\%$ for Pb, to $11 \pm 3\%$ for carbon), and the empty target background (25% for lead, to 11% for carbon). There was no correction for the radiative smearing of Q^2 and ν of hadronic events. The radiative smearing correction should not depend on nucleon number except for the shadowing effect itself. Also shown in Figure 2 are the hydrogen data from earlier μp scattering experiments with this apparatus, where the data used are similarly uncorrected for radiative smearing and we have assigned a 10% relative normalization error to the hydrogen data. The straight lines in Figure 2 represent power law fits to the nuclear data only. The slope parameter $(\rho-1)$ of these fits is given in Table 1 together with those from fits which include the hydrogen data points from the earlier experiment. Values of this parameter significantly less than zero indicate shadowing. The data exhibit shadowing at low Q^2 , with and without the inclusion of the earlier hydrogen measurement.

Grammer and Sullivan² have suggested that the shadowing effect be parameterized as:

$$\frac{A_{\text{eff}}}{A} = \frac{\sigma(A)}{A\sigma(1)} = G(R/\ell) \quad (2)$$

where A_{eff} is the effective number of nucleons participating in the

interaction⁷ for a target of nucleon number A , and σ is the total hadronic virtual photon cross sections for A nucleons. The shadowing parameter G may be defined in terms of the nuclear radius R , and the virtual photon mean free path in nuclear matter, ℓ . We have normalized our data to the hydrogen data⁸ and fit these values of A_{eff}/A to the form of $G(R/\ell)$ given in Ref. 2 for the case of uniform density, leaving the virtual photon mean free path as the variable parameter. The results of these fits are given in Table 2. A typical hadronic mean free path in nuclear matter at these energies is ~ 2.5 Fm; thus for $Q^2 < 1 \text{ GeV}^2$ the data are consistent with hadronic behavior, whereas at large Q^2 the mean free path is larger than the nuclear diameter and the shadowing effect is diminished. The errors on ℓ include both the systematic normalization error assigned to the hydrogen data and the statistical error in the cross section measurements on nuclei.

Figure 3 shows A_{eff}/A for C, Cu, and Pb targets, along with results from a recent high energy photoproduction experiment⁹ at 60 and 135 GeV. We note that at these high energies, the hydrogen cross section is slowly rising, while the nuclear photoproduction cross sections are falling as a function of ν . The errors shown are statistical only, and there may be an overall systematic error of $\pm 10\%$ due to the relative normalization of the hydrogen data. The shadowing effect we observe, while consistent at low Q^2 with the high energy photoproduction result, persists to larger Q^2 than most earlier

low ν electroproduction results. However, the lower energy experiments are inconsistent among themselves.^{10,11,12,13,14}

In conclusion, we observe shadowing for $Q^2 < 1 \text{ GeV}^2$ and see shadowing diminish at larger Q^2 for the ν range (40-200) GeV. In the context of generalized vector meson dominance theories (GVMD), this data provides evidence that higher mass vector mesons than the ρ meson participate in shadowing at these high energies.

We thank the Fermilab staff, the staff at the Rutherford Lab Computing Center, Dr. W.S.C. Williams of Oxford University and students S. Schochet, A. Karpovsky, and G. Denis at Harvard and Dr. R. Milburn of Tufts University for their contributions to this work. We also thank Dr. G. Grammer for the use of his radiative computer calculation codes and useful discussion.

Present Address:

- ^o Mathematics Department, Univ. of Wisconsin, Madison, WI 53706
- ^s Stanford Linear Accelerator Center, Menlo Park, CA 94305
- ^ξ Bell Telephone Laboratories, Naperville, IL 60540
- ^{††} Hughes Aircraft Corporation, Los Angeles, CA 90009
- ^Δ C.R.A. Services, Ltd., Melbourne, Australia 3001
- ^η High Energy Physics Laboratory, Harvard Univ., Cambridge, MA
- [~] Physics Dept., Vanderbilt Univ., Nashville, TN 37235
- ⁺ Work supported in part by the U.S. Department of Energy
- ^{**} Work supported in part by the National Science Foundation
- ^{*} Work supported in part by the Science Research Council (UK).

REFERENCES

1. T. H. Bauer, et al., Rev. Mod. Phys., 50, 261 (1978).
2. G. Grammer Jr. and J.D. Sullivan in Electromagnetic Interactions of Hadrons, Vol. 2, ed. A. Donnachie and G. Shaw, Plenum, 1978, pp. 135-351.
3. B. A. Gordon et al., Phys. Rev. D., 20, 2645 (1980) and B. A. Gordon, PhD. Thesis, Harvard Univ. (1978) and J. Proudfoot, PhD. Thesis, Oxford Univ. (1979).
4. W. A. Loomis et al., Phys. Rev. D., 19, 2543 (1979).
5. J. J. Aubert et al., Phys. Lett. 95B, 306 (1980).
6. R. L. Ford and W. R. Nelson, SLAC Pub. 210 (1978).
7. The n-p cross section difference at these high energies is <1% and has been neglected in computing A_{eff} .
8. To obtain the hydrogen cross section in the region $Q^2 < .3 \text{ GeV}^2$, a fit was made to the data of Ref. 3 and included the $Q^2 = 0$ measurement of D. O. Caldwell et al., Phys. Rev. Lett. 40, 1222 (1978).
9. D. O. Caldwell et al., Phys. Rev. Lett., 42, 553 (1979).
10. J. Eickmeyer, et al., Phys. Rev. Lett. 36, 289 (1976) and S. Michalowski, et al., Phys. Rev. Lett., 39, 737 (1977).
11. J. Bailey, et al., Nucl. Phys. B151, 367 (1979).
12. S. Stein et al., Phys. Rev. D12, 1884 (1975).
13. M. May et al., Phys. Rev. Lett., 35, 407 (1971).
14. M. Miller et al., submitted to the Physical Review (1981).

TABLE I

PARAMETER $(\rho-1)$ IN THE FIT $\frac{\bar{\sigma}(A)}{A} = cA^{(\rho-1)}$		
$Q^2(\text{GeV}^2)$	$(\rho-1)$ <u>This Expt. Only</u>	$(\rho-1)$ <u>This Exp. & Hydrogen Data</u>
0.01 - 0.3	$-0.061 \pm .025$	$-0.084 \pm .020$
0.3 - 1.0	$-0.113 \pm .036$	$-0.107 \pm .024$
1.0 - 3.0	$-0.049 \pm .052$	$-0.090 \pm .027$
3.0 - 10.0	$-0.023 \pm .042$	$-0.030 \pm .023$
10.0 - 30.0	$-0.034 \pm .095$	$-0.036 \pm .037$

TABLE II

FITTED VIRTUAL PHOTON MEAN FREE PATH

Q^2	l	χ^2/df
.01-0.3	$5.03^{+2.08}_{-1.20}$	1.9
0.3-1.0	$3.45^{+1.15}_{-0.72}$	3.2
1.0-3.0	$4.41^{+2.48}_{-1.25}$	0.6
3.0-10.0	$14.08^{+51.2}_{-6.4}$	0.3
10.0-30.0	$10.48^{+47.0}_{-5.41}$	0.4

(R(C) \simeq 2.6 fm, R(Cu) \simeq 4.5 fm, R(Pb) \simeq 6.6 fm)

FIGURES

1. The CCM spectrometer (top view): BS are beam defining counters, HV is a halo veto wall, PC are multiwire proportional chambers, SC are spark chambers, H, G, M, and P are scintillation counter hodoscopes, HA is a 2m steel muon identifier and V is the beam veto. CCM is the Chicago Cyclotron Magnet and MI is the downstream magnet iron.
2. Average virtual photon total hadronic cross section for various $(Q^2 - \nu)$ ranges as a function of A.
3. A_{eff}/A as a function of Q^2 for targets of C, Cu and Pb. Also shown are data from a high energy photoproduction experiment (Reference 9).

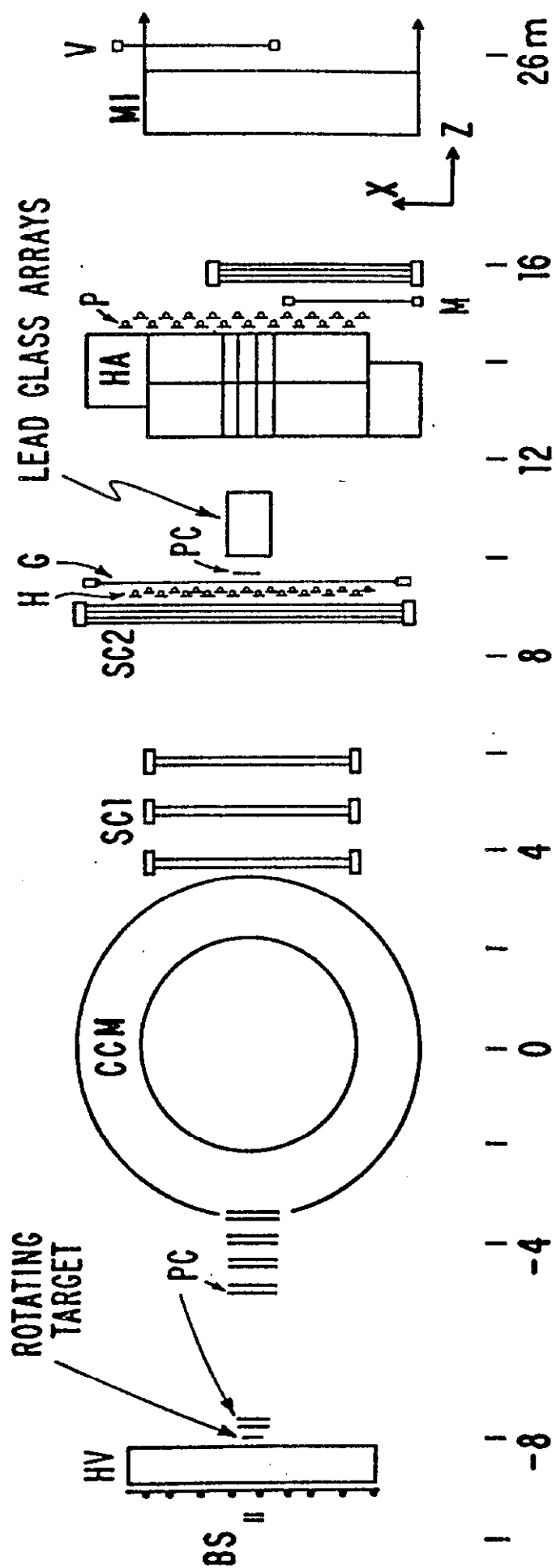


Fig. 1

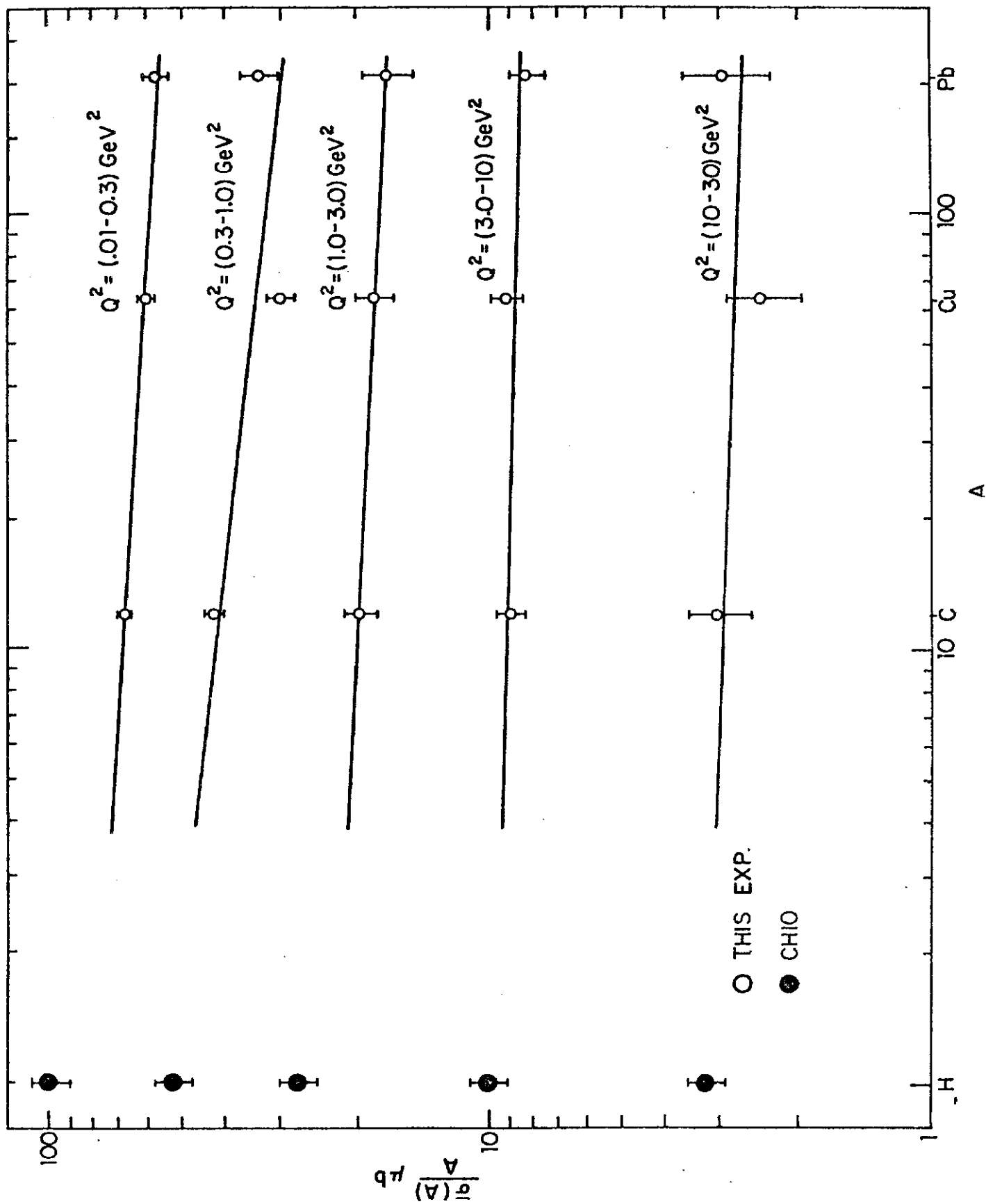


Fig. 2

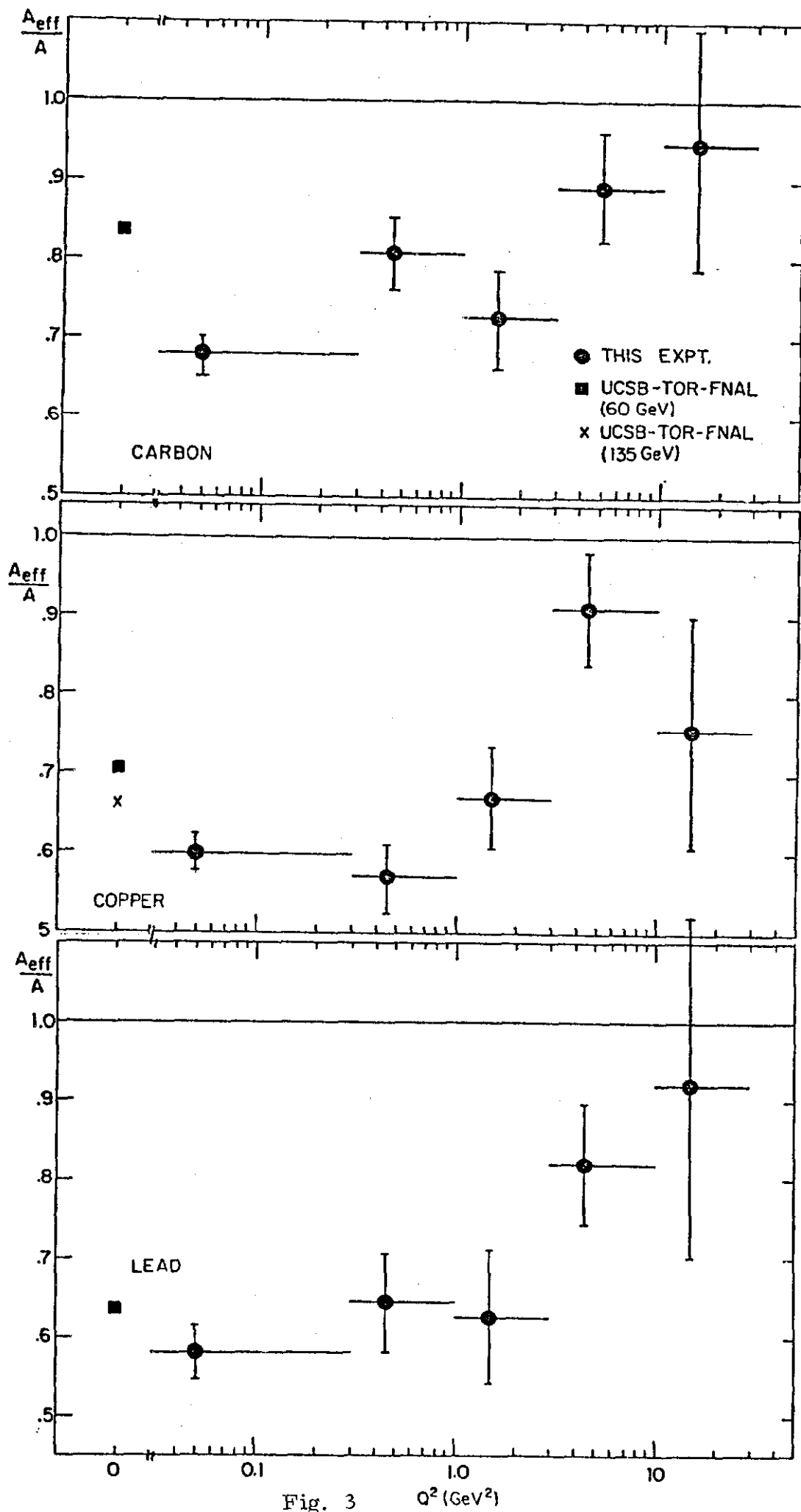


Fig. 3 Q^2 (GeV²)